HHS Public Access

Author manuscript

Retina. Author manuscript; available in PMC 2017 June 01.

Published in final edited form as:

Retina. 2016 June ; 36(6): 1153–1161. doi:10.1097/IAE.0000000000000842.

Real-time full-depth visualization of posterior ocular structures: comparison between Full Depth Imaging Spectral Domain OCT and Swept Source OCT

Giulio Barteselli, MD[1,2], **Dirk-Uwe Bartsch, PhD**[1], **Robert N Weinreb, MD**[1], **Natalia Camacho, MD**[1], **Joseph T Nezgoda, MD**[1], **Amir H Marvasti, MD**[1], and **William R Freeman, MD**[1]

[1]Department of Ophthalmology, Shiley Eye Center, University of California San Diego, La Jolla CA

[2]Genentech Inc, South San Francisco CA

Abstract

Purpose—To compare the real-time visualization of vitreoretino-choroidal structures using Full Depth Imaging (FDI) spectral domain optical coherence tomography (SD-OCT) and swept source (SS)-OCT.

Methods—Foveal scans using both FDI SD-OCT (Heidelberg Spectralis) and SS-OCT (Topcon DRI OCT-1) were obtained in 40 normal eyes, 40 eyes with macular pathologies, and 40 eyes with glaucoma. FDI SD-OCT images were obtained by manually enhancing the vitreoretinal interface first and then the choroid, while averaging each OCT B-scan 100 times. SS-OCT images were obtained by averaging each B-scan 96 times. After masking and randomly mixing the original OCT images, two independent physicians graded visualization of the premacular bursa, interdigitation zone line, and chorio-scleral boundary, as well as sharpness of choroidal structures.

Results—A real-time full-depth image of vitreoretino-choroidal structures was successfully achieved with FDI SD-OCT in 118 cases (98.3%) and with SS-OCT in 45 cases (37.5%, $p<0.001$). FDI SD-OCT imaging was superior to SS-OCT imaging in visualizing the anterior border of the premacular bursa in 109 eyes (90.8%), with average grading of 1.63 ± 0.53 for the FDI SD-OCT and 0.39 ± 0.52 for the SS-OCT ($p<0.001$). SS-OCT was similar to FDI SD-OCT in visualizing the chorio-scleral boundary in 108 eyes (90.0%), with average grading of 1.81 ± 0.39 for the SS-OCT and 1.78 ± 0.38 for the FDI-OCT ($p=0.566$). The visualization of the interdigitation zone line was identical in the two imaging instruments ($p=1.000$). The sharpness of the choroidal structures was greater with SS-OCT than with FDI-OCT ($p<0.001$).

[§]Corresponding author: William R. Freeman, MD, University of California at San Diego, Shiley Eye Center, 0946, 9415 Campus Point Drive, La Jolla, CA 92037; ; Email: freeman@eyecenter.ucsd.edu; phone (858) 534-3513.

Financial disclosures:

- Giulio Barteselli is a full-time employee at Genentech, Inc.
- Robert N Weinreb receives research support from Carl-Zeiss Meditec, Heidelberg Engineering, Kowa, Nidek, and Topcon, and is a consultant to Carl-Zeiss Meditec and Topcon.
- The other authors have no financial interests to disclose.

Conclusion—Manual double-enhancing FDI technique using SD-OCT provided a good compromise between vitreous and retino-choroidal structures visualization in real time during scanning procedure. In contrast, SS-OCT imaged well fine choroidal details. Appropriate OCT technology and software should be selected according to its application in clinical settings.

Keywords

spectral domain optical coherence tomography; SD-OCT; swept source optical coherence tomography; SS-OCT; full depth imaging; combined depth imaging; vitreous imaging; choroid imaging; choroidal thickness

Introduction

Since its introduction in ophthalmology in 1991 optical coherence tomography (OCT) technology has developed rapidly and has become an essential tool for visualization and management of many ocular diseases. Higher scan rate, shorter acquisition time, finer axial resolution, and variable wavelengths have allowed faster image capturing, lower noise, and deeper tissue penetration. This has translated into better resolution cross-sectional imaging of the posterior ocular structures. Spectral domain (SD)-OCT is currently the most widely used OCT technology. With the use of 820- to 880-nm probing light and scan rate of 52,000 Hz or greater, the SD-OCT provides excellent imaging of the vitreo-retinal interface and retina.

Due to increased interest in non-invasive choroidal imaging with OCT, other methods have recently been developed to enhance and measure deeper structures such as the choroid. These methods include the enhanced depth imaging (EDI) technique using SD-OCT technology and the new generation swept source (SS)-OCT. The EDI acquisition software on SD-OCT devices automatically places the choroid close to the zero delay line to maximize sensitivity of the outer border of the choroid.[1] Alternatively, using longer center wavelength (1,040 to 1,060 nm) and higher scan rate (100,000 Hz),[2] SS-OCT does not suffer from loss of sensitivity across the imaging depth range and the tissue of interest does not need to be positioned close to the zero delay to enhance sensitivity. These OCT technologies allow deeper penetration into the choroid, however the simultaneous visualization of the preretinal vitreous structures is limited because the ratio of signal produced by the vitreous is very small compared to that produced by the retina or choroid. One can quite easily adjust brightness and contrast of the scans with the built-in image review software of the OCT device after image acquisition, however the extent of enhancement is limited because the software does not allow for local image adjustment, i.e. adjustment of only a selected portion of the image. In case of drastic changes in brightness/contrast due to low signal from the vitreous in the original image, the preretinal vitreous structures become much more visible. However, because the enhancement affects the whole OCT image, the retina and choroid can potentially become over-exposed with loss of fine structural details. Therefore one must find an acceptable compromise between vitreous and retino-choroidal enhancement to maintain overall structural details. Alternatively, after acquiring and exporting OCT images one can selectively enhance only the vitreous with the use of

dedicated third party software. However, this selective vitreous-enhancement process using external software can't be performed in clinic in a timely fashion.

To overcome this potential issue, our group has previously described a manual double-enhancing technique that allows simultaneous in-vivo visualization of both superficial and deep posterior structures into a single OCT image using the Spectralis HRA+OCT (Heidelberg Engineering, Heidelberg, Germany).[3, 4] The “Full Depth Imaging” (FDI) technique, also called “Combined Depth Imaging” (CDI) technique,[3-5] involves a live process that first enhances the vitreo-retinal interface using the conventional SD-OCT modality and then the choroid using the EDI-OCT modality, while averaging multiple OCT scans using the active eye-tracking feature of the Spectralis. This allows for a single-image full-depth evaluation of the posterior structures (including vitreous, retina, and choroid) in real time while imaging patients and without using multiple OCT modalities or external software for image processing.

The purpose of the present study was to analyze the real-time full-depth visualization of macular structures as assessed by the FDI SD-OCT technique compared to the SS-OCT technology without the use of post-image processing. Specifically, the aims were 1) to determine whether the ability to obtain a full-depth visualization of posterior vitreoretino-choroidal structures was different between the two techniques, and 2) to determine whether the ability to visualize three specific structures including the anterior border of the premacular bursa, the interdigitation zone line, and the outer border of the choroid were different between the two techniques.

Methods

Subjects

This was a prospective comparative study of 60 patients (120 eyes) seen at the Shiley Eye Center at University of California San Diego (UCSD, La Jolla, CA) over a 2-month period. The study population included 20 healthy volunteers, 20 subjects with macular disease, and 20 patients with glaucoma. Healthy subjects and patients with glaucoma were a cohort of consecutive participants of a prospective longitudinal study, the Diagnostic Innovations in Glaucoma Study (DIGS) at UCSD, designed to evaluate optic nerve structure and visual function in glaucoma.[6] Patients with macular diseases were consecutively recruited in a retina clinic. Exclusion criteria included posterior vitreous detachment detected by indirect ophthalmoscopy, myopia of -5 diopters or more, hyperopia of +3 diopters or more, and the presence of any ocular disease other than a macular disease or glaucoma. Eyes with any media opacities that could significantly affect the quality of the scans were also excluded. Informed consent was obtained from all study participants. The study protocol adhered to the tenets of the Declaration of Helsinki and was approved by the institutional review board of UCSD.

OCT Imaging

After pupillary dilation, OCT examinations were performed by a single experienced physician (G.B.) who scanned all participants, bilaterally, with both the Spectralis and the

Topcon Deep Range Imaging (DRI) OCT-1 Atlantis 3D SS-OCT (Topcon Medical Systems, Oakland, N.J.), which is currently investigational in the United States. The two scans were obtained within 5 minutes, with the first scanning device randomly chosen. A 9-mm horizontal line scan passing through the fovea was obtained for each eye with an internal fixation target, using the best-quality settings of the machines. An attempt was made to obtain the highest quality scan for each patient.

- The Spectralis uses an 870-nm central wavelength and a 40,000-Hz scan rate, yielding a 5-μm axial resolution in tissue. The total scan depth is 1.9 mm. The device was set to perform a 9-mm high-resolution horizontal B-scan, with the averaging system set to the maximum (100 B-scans). The double-enhanced FDI SD-OCT image was obtained as previously described.[3, 4] After positioning the OCT B-scan in the middle of the screen, the operator shifted the focus of the instrument slightly toward plus values to highlight the posterior vitreous architecture. The averaging system of the device using the conventional OCT software was then activated; after reaching at least 80% of the averaging (at least 80 of 100 B-scans), the operator manually activated the EDI acquisition software. The FDI SD-OCT image that resulted was captured as soon as a good-quality image was visualized. To be accepted, all FDI SD-OCT images had to have signal strength of 25 dB or more; the signal strength was automatically reported for each image.
- The DRI-OCT uses a 1,050-nm central wavelength and a 100,000-Hz scan rate, yielding an 8-mm axial resolution in tissue. The total scan depth is 2.6 mm. The device was set to perform a 9-mm horizontal B-scan using the vitreous reference position, with the averaging system set to the maximum (96 B-scans). To be accepted, all SS-OCT images had to have an image quality score of 45 or more; this score was automatically reported for each image. The quality score of the DRI-OCT is in arbitrary units.

OCT analysis

The original FDI SD-OCT and SS-OCT images for each eye were saved as maximum quality JPEG image files in native resolution and without brightness/contrast modification. All images then were masked by an independent operator (D-U.B.), removing features identifying OCT scan method and patient information, and then were mixed randomly. Two independent masked physicians (J.T.N., N.C.) reviewed each image on the same monitor with same resolution at different time points and evaluated images using a previously used method.[4] First, they evaluated the ability to visualize a full-depth image of the vitreoretino-choroidal structure. Then, they evaluated visualization of single structures; in particular, they graded visualization of the inner border of the premacular bursa, visualization of the interdigitation zone line, and visualization of the chorio-scleral boundary separately. Grade 0 indicated that the structure was not seen, grade 1 indicated that the structure was barely seen, and grade 2 indicated that the structure was clearly seen. Finally, they evaluated the sharpness of choroidal structures by qualitative comparison of the two OCT images for each eye; the physicians judged which of the two masked images showed best the choroidal details. In case of disagreement, a third physician (G.B.) was consulted to achieve an acceptable result.

Statistical analysis

The interobserver agreement for the grading of the inner border of the premacular bursa, interdigitation zone line, and chorio-scleral boundary was assessed using the Cohen k. Comparison for significant difference of grading score between FDI-OCT and SS-OCT images was analyzed using the paired t test for normal distribution data or Wilcoxon signed-rank test for non-normal distribution data. Statistical analysis was performed using SPSS statistical software version 20.0 (SPSS Inc, Chicago, Illinois, USA). A p value less than 0.05 was considered to be statistically significant.

Results

All 120 eyes from the 60 patients ultimately underwent evaluation based on ability to obtain high-quality OCT images with either OCT modality. The mean age of the patients was 50 years (range, 25 to 75 years). Macular pathology among patients included dry age-related macular degeneration (AMD; 12 eyes), wet AMD (8 eyes), diabetic macular edema (14 eyes), macular teleangectasia type 2 (4 eyes), and vitreo-macular traction (2 eyes).

The agreement between observers in grading visualization of OCT features was high (overall k = 0.75; k = 0.71 for the inner border of the premacular bursa; k = 1.00 for the interdigitation zone line; k = 0.69 for the chorio-scleral boundary). Results of the average grading of the inner border of the premacular bursa, interdigitation zone line, and chorio-scleral boundary are shown in Figure 1. A full-depth image of vitreoretino-choroidal structures was successfully achieved with FDI SD-OCT in 118 cases (98.3%) and with SS-OCT in 45 cases (37.5%, $p<0.001$).

The anterior border of the premacular bursa was detected in 117/120 cases with FDI SD-OCT (98%) and in 45/120 cases with SS-OCT (38%, $p<0.001$) (Figure 2). The FDI SD-OCT was superior to the SS-OCT in visualizing the anterior border of the premacular bursa in 109 eyes (90.8%), while the 2 machines performed similarly for the remaining eyes. More precisely, the average grading for the anterior border of the premacular bursa was 1.63 ± 0.53 for the FDI SD-OCT and 0.39 ± 0.52 for the SS-OCT ($p<0.001$).

The chorio-scleral boundary was detected in all cases with both FDI SD-OCT and SS-OCT. Compared to the FDI SD-OCT, the SS-OCT was similar in the visualization of the chorio-scleral boundary in 108 eyes (90.0%), superior in 7 eyes, and inferior in 5 eyes. More precisely, the average grading for the chorio-scleral boundary was 1.81 ± 0.39 for the SS-OCT and 1.78 ± 0.38 for the FDI SD-OCT ($p=0.566$). The visualization of the interdigitation zone line was identical between the two OCT techniques ($p=1.000$).

In subgroups analysis, the visualization of the anterior border of the premacular bursa was consistently better using FDI SD-OCT than SS-OCT ($p<0.001$), while the visualization of the chorio-scleral boundary was similar between the two OCT techniques ($p=0.564$ for normal eyes, $p=0.564$ for eyes with AMD, and $p=0.414$ for eyes with glaucoma). The sharpness of choroidal structures was greater with SS-OCT than with FDI SD-OCT ($p<0.001$).

Selected case reports

Case 1—A 72-year-old woman with wet AMD underwent multiple intravitreal injections of bevacizumab before inclusion in the study. Her best-corrected visual acuity was 20/80 and she was complaining of persistent metamorphopsias. Both FDI SD-OCT and SS-OCT detected a fibrovascular pigment epithelium detachment with serous subretinal fluid involving the macula (Figure 3). The choroid was clearly imaged with both OCT machines; on the contrary the FDI SD-OCT nicely showed presence of the premacular bursa with vitreomacular traction that was barely evident on the SS-OCT image. Considering the established influence of the vitreomacular adhesion in the treatment of wet AMD,[7] this finding could have had a clinical importance in the management of such patient.

Case 2—A 46-year old woman was recruited as a healthy volunteer. Her best-corrected visual acuity was 20/20 in OU and she had no visual complains. The premacular bursa was clearly detected only on the FDI SD-OCT image (Figure 4). Both OCT machines showed the five layers of the choroid, including Bruch's membrane, choriocapillaris, two vascular layers (Haller's and Sattler's), and the suprachoroidal space. However, the choroidal structures were sharper in the SS-OCT image compared to the FDI SD-OCT image.

Discussion

In the present study we compared the ability of two different OCT devices in imaging posterior ocular structures in real time while scanning patients, and we compared the quality of visualization of specific structures such as the premacular bursa, interdigitation zone line, and chorio-scleral boundary on the original OCT images without using post-image processing. With the use of the novel FDI technique, we found superior ability of the Spectralis compared to the SS-OCT in providing a real-time full-depth image of the vitreoretino-choroidal structures. In addition, greater visualization of the vitreous was obtained using the former, whilst the ability of visualizing the full-depth image of the choroid was similar between the two OCT devices. Nevertheless, the SS-OCT showed sharper visualization of fine choroidal details. Similar trends were seen when analyzing data across the spectrum of normal subjects, patients with macular disease, or patients with glaucoma.

Swept-source OCT technology has been developed to improve both vitreous and choroidal imaging because it maintains high sensitivity over a much longer imaging depth range than SD-OCT, and long wavelengths provide better immunity to ocular opacities.[8] One of the features of SD-OCT is the decrease in sensitivity with axial distance. In contrast, SS-OCT does not suffer from this decrease. The greater scanning speed of SS-OCT compared to SD-OCT technology allows faster OCT examination of the patients. However, the width of the 1,050 nm water absorption window limits the achievable axial resolution.[9] In addition, axial resolution and imaging contrast of the anterior retina layers is linearly dependent on the wavelength of the light. Thus, imaging in the 820- to 880-nm range in SD-OCT permits higher axial resolution and appears to provide higher inner retinal layer contrast than 1,050 nm.[10] The current study demonstrated that the double enhancement of vitreous and choroid, using the FDI technique with SD-OCT imaging, allows for acquisition of good quality full-

depth images in significantly more cases compared with those acquired using SS-OCT imaging. One possible explanation for such a finding is that the higher axial resolution of the Spectralis SD-OCT coupled with the automatic real-time averaging feature allow for high-contrast noise-reduced images, improving visualization of structures in these areas without the need for post-image processing. The cSLO-to-OCT image registration and eye-tracking feature of the SD-OCT allow for averaging of individual B-scans in the same exact location using both standard and EDI modes. Such a feature allows for optical defocusing during the acquisition process in standard mode, maximizing the imaging depth and brightness into the vitreous. With the FDI technique, after many images have been averaged using parameters for optimal vitreous imaging, EDI mode can be activated to optimize scan parameters for choroidal imaging. The final construct of the optically defocused standard mode combined with the EDI mode allows for optimized image contrast in the vitreo-retinal interface, retina, and chorio-scleral interface using SD-OCT. Although SS-OCT technology improved choroidal imaging, vitreous imaging is still problematic. The illumination beam of the SS-OCT is relatively defocused in the vitreous cavity, the signal produced by the vitreous is weak, and the ratio of signal produced by the vitreous is very small compared to that produced by the retina. Therefore, the visualization of both vitreous and retina in a grayscale image is difficult.[11] As recently shown, the "*dynamic focusing with windowed averaging*" technique on SS-OCT can be a partial solution for this; this technique constructs an image in a limited part, or window, of the scanned region from 96 scans, actively focusing the beam. However, the resultant image still has a great disparity between the signal strength from the vitreous as compared with the retina.[11]

Optical coherence tomography images are typically displayed in logarithmic scale in order to accommodate the large dynamic range of the backscattered light from vitreo-retinal structures. Since a limited number of grey scale levels can be displayed in an image and perceived by the human eye, logarithmic scale display is used to compress the dynamic range, resulting in loss of contrast within specific tissue structures.[8] Using standard logarithmic scale display without any post-image processing for enhancing vitreous, Stanga et al. have recently reported by the use of SS-OCT a 57% prevalence of the premacular bursa in the general population; after the age of 60 years, it was detected in only 30% of people.[12] It is possible that the authors underestimated the prevalence, missing cases with a more anterior bursa, because a vitreous-enhancing image modification was not performed. Indeed, using the FDI technique on SD-OCT we were able to image the anterior border of the premacular bursa in 98% of the eyes. This is extremely close to the results of other SS-OCT studies that found 100% prevalence of premacular bursa after enhancing vitreous.[13, 14] To overcome this suboptimal real-time visualization of the vitreous structures using SS-OCT or conventional SD-OCT, several image-processing techniques are available to enhance preretinal structures after capturing B-scan images. In the majority of the published studies, investigators have used a windowing technique (the *"vitreous windowing display"*) to process standard logarithmic scale images, adjusting brightness/contrast of the whole image using built-in image review software of the OCT device after image acquisition;[13-16] although the signal from the vitreous became dramatically enhanced, this potentially resulted in over-exposure of the retinal and choroidal tissues and thus in loss of fine structural details. Other investigators have used a high-dynamic-range technique (the *"HDR*

display") to convert OCT images to a displayable range while preserving contrast, brightness, and fine details using external software.[8] However, they found that the HDR display provided lower sensitivity for vitreous analysis when compared to the vitreous windowing display.[8] Finally, local image adjustment can be performed using the "*adaptive histogram equalization*". In this method, local regions of an image are transformed in brightness/contrast according to a selectable neighborhood of local pixel values; local image gain is varied according to the cumulative distribution function of the region. This method, that can be performed with a dedicated third party software, has been recently shown to be extremely useful in improving display of the vitreous without affecting quality of the retinal imaging.[11] These multiple techniques may be useful to enhance the posterior vitreous architecture, however the image modification process can't be performed in real time during scanning. In addition, the use of external software such as Photoshop or ImageJ is impractical in clinic and also time-consuming for physicians. Finally, the clinical truthfulness of images manipulated with third party software may be questionable.[17] On the contrary, the FDI technique allows for real-time enhancement of the vitreous during the initial stage of acquisition (shifting the focus of the SD-OCT slightly toward plus values and activating the image averaging system) and then the choroid in the latter stage (activating the EDI mode during averaging) while scanning a patient. For these reasons, in the present study we neither needed to adjust brightness and contrast of the OCT scans after acquisition, or use external software to locally modify them. Instead, we evaluated original OCT images taken in real time with the two OCT devices. Using this manual double enhancement of vitreous and choroid, we demonstrated that the FDI technique allowed better real-time visualization of the posterior vitreous architecture in more than 90% of the cases compared with conventional SS-OCT imaging.

The current study was not designed to analyze differences in choroidal thickness measurements, however recent studies have shown that thickness measurements were similar if performed with either SD-OCT or SS-OCT.[18, 19] For clinical purpose of visualizing choroidal borders for choroidal thickness measurement we demonstrated the two machines are similar, although in a few cases the SS-OCT allowed better detection of the chorio-scleral border. Moreover, we did notice greater sharpness of choroidal details using the SS-OCT; this was likely a result of superior detection efficiency and sensitivity roll-off performance of the SS-OCT. For research purposes, a better recognition of choroidal vasculature sublayers may be important for understanding the choroidopathy in the pathophysiology of chorio-retinal diseases. For example, performing en-face OCT or OCT-angiography by using SS-OCT devices, some investigators were able to reconstruct choriocapillaris and choroidal microvasculature visualization that was consistent with known architectural morphology from early histological findings.[20, 21] Moreover, using a 1,060 nm SD-OCT prototype, other investigators have recently shown significant changes in choroidal, Haller's and Sattler's layer thickness in relation to the progression of age-related macular degeneration.[22] Using standard 820- to 880-nm SD-OCT devices, the recognition and delineation of choroidal vasculature sublayers is a challenge.

There are some limitations/disadvantages of the FDI SD-OCT technique. This technique currently is possible only with the Heidelberg Spectralis; no other commercial SD-OCT device is able to simultaneously double enhance the vitreous and choroid, to track eye

movements, and to perform image averaging. Also, at the current time it must be performed manually by clicking a button to switch between averaging centered on the anterior layers and posterior layers. The full-depth image can be obtained only on a single linear B-scan, whereas the automatic image capture when performing a raster scan currently does not allow manual activation of the EDI mode; therefore, a 3-dimensional reconstruction of the posterior structures is not possible. The FDI SD-OCT image takes a few seconds to be acquired, due to the necessity of averaging a high number of B-scan images; therefore, it is difficult to perform in patients with poor fixation. Finally, the longer wavelength used by the SS-OCT is less likely to be absorbed by lens opacities compared to the shorter wavelength of the SD-OCT.

In conclusion, this prospective study demonstrated that double-enhancing FDI technique using SD-OCT provided a good compromise between vitreous and choroid visualization while scanning eyes without significant media opacities. Using such technique, image modification processes with built-in image review software or third party software are not needed because adequate display of vitreous, retina, and choroid is obtained in real time while scanning an eye with no risk of image over-exposure. With its enhanced detection efficiency and sensitivity roll-off performance, first generation SS-OCT visualized well details of choroidal sublayers, but only partially visualized the posterior vitreous architecture without using post-image processing that may alter the image quality or be burdensome for physicians. For clinical purposes of visualizing choroidal borders for choroidal thickness measurement, the two technologies appeared similar. Appropriate OCT technology and software should be selected according to its applications in clinical settings.

Acknowledgments

Financial support: This study was supported by NIH grant R01EY016323, NEI vision core grant P30EY022589, and an unrestricted fund from the Research to Prevent Blindness to the Department of Ophthalmology, University of California, San Diego. The funding organizations had no role in the design or conduct of this research.

References

1. Spaide RF, Koizumi H, Pozzoni MC. Enhanced depth imaging spectral-domain optical coherence tomography. Am J Ophthalmol. 2008; 146(4):496–500. [PubMed: 18639219]
2. Potsaid B, Baumann B, Huang D, et al. Ultrahigh speed 1050nm swept source/Fourier domain OCT retinal and anterior segment imaging at 100,000 to 400,000 axial scans per second. Opt Express. 2010; 18(19):20029–48. [PubMed: 20940894]
3. Barteselli G, Bartsch DU, Freeman WR. Combined depth imaging using optical coherence tomography as a novel imaging technique to visualize vitreoretinal choroidal structures. Retina. 2013; 33(1):247–8. [PubMed: 23138345]
4. Barteselli G, Bartsch DU, El-Emam S, et al. Combined depth imaging technique on spectral-domain optical coherence tomography. Am J Ophthalmol. 2013; 155(4):727–32. 32 e1. [PubMed: 23253912]
5. Mahendradas P, Madhu S, Kawali A, et al. Combined depth imaging of choroid in uveitis. Journal of Ophthalmic Inflammation and Infection. 2014; 4:18. [PubMed: 26530343]
6. Sample PA, Girkin CA, Zangwill LM, et al. The African Descent and Glaucoma Evaluation Study (ADAGES): design and baseline data. Arch Ophthalmol. 2009; 127(9):1136–45. [PubMed: 19752422]

7. Mayr-Sponer U, Waldstein SM, Kundi M, et al. Influence of the vitreomacular interface on outcomes of ranibizumab therapy in neovascular age-related macular degeneration. Ophthalmology. 2013; 120(12):2620–9. [PubMed: 23870300]

8. Liu JJ, Witkin AJ, Adhi M, et al. Enhanced vitreous imaging in healthy eyes using swept source optical coherence tomography. PLoS One. 2014; 9(7):e102950. [PubMed: 25036044]

9. Hariri S, Moayed AA, Dracopoulos A, et al. Limiting factors to the OCT axial resolution for in-vivo imaging of human and rodent retina in the 1060 nm wavelength range. Opt Express. 2009; 17(26): 24304–16. [PubMed: 20052141]

10. Chen Y, Burnes DL, de Bruin M, et al. Three-dimensional pointwise comparison of human retinal optical property at 845 and 1060 nm using optical frequency domain imaging. J Biomed Opt. 2009; 14(2):024016. [PubMed: 19405746]

11. Spaide RF. Visualization of the posterior vitreous with dynamic focusing and windowed averaging swept source optical coherence tomography. Am J Ophthalmol. 2014; 158(6):1267–74. [PubMed: 25174895]

12. Stanga PE, Sala-Puigdollers A, Caputo S, et al. In vivo imaging of cortical vitreous using 1050-nm swept-source deep range imaging optical coherence tomography. Am J Ophthalmol. 2014; 157(2): 397–404 e2. [PubMed: 24439443]

13. Itakura H, Kishi S, Li D, Akiyama H. Observation of posterior precortical vitreous pocket using swept-source optical coherence tomography. Invest Ophthalmol Vis Sci. 2013; 54(5):3102–7. [PubMed: 23599325]

14. Schaal KB, Pang CE, Pozzoni MC, Engelbert M. The premacular bursa's shape revealed in vivo by swept-source optical coherence tomography. Ophthalmology. 2014; 121(5):1020–8. [PubMed: 24507856]

15. Pang CE, Schaal KB, Engelbert M. Association of Prevascular Vitreous Fissures and Cisterns with Vitreous Degeneration as Assessed by Swept Source Optical Coherence Tomography. Retina. 2015

16. Li D, Kishi S, Itakura H, et al. Posterior precortical vitreous pockets and connecting channels in children on swept-source optical coherence tomography. Invest Ophthalmol Vis Sci. 2014; 55(4): 2412–6. [PubMed: 24609625]

17. Rossner M, Yamada KM. What's in a picture? The temptation of image manipulation. J Cell Biol. 2004; 166(1):11–5. [PubMed: 15240566]

18. Adhi M, Liu JJ, Qavi AH, et al. Choroidal analysis in healthy eyes using swept-source optical coherence tomography compared to spectral domain optical coherence tomography. Am J Ophthalmol. 2014; 157(6):1272–81 e1. [PubMed: 24561169]

19. Ikuno Y, Maruko I, Yasuno Y, et al. Reproducibility of retinal and choroidal thickness measurements in enhanced depth imaging and high-penetration optical coherence tomography. Invest Ophthalmol Vis Sci. 2011; 52(8):5536–40. [PubMed: 21508114]

20. Motaghiannezam SM, Koos D, Fraser SE. Differential phase-contrast, swept-source optical coherence tomography at 1060 nm for in vivo human retinal and choroidal vasculature visualization. J Biomed Opt. 2012; 17(2):026011. [PubMed: 22463043]

21. Choi W, Mohler KJ, Potsaid B, et al. Choriocapillaris and choroidal microvasculature imaging with ultrahigh speed OCT angiography. PLoS One. 2013; 8(12):e81499. [PubMed: 24349078]

22. Esmaeelpour M, Ansari-Shahrezaei S, Glittenberg C, et al. Choroid, Haller's, and Sattler's Layer Thickness in Intermediate Age-Related Macular Degeneration With and Without Fellow Neovascular Eyes. Invest Ophthalmol Vis Sci. 2014; 55(8):5074–80. [PubMed: 25052997]

Summary statement

We analyzed the real-time full-depth visualization of vitreoretinal-choroidal structures using the novel Full Depth Imaging (FDI) SD-OCT technique compared to the SS-OCT technology. Double-enhancing FDI SD-OCT provided a good compromise between vitreous and choroid visualization in real time. SS-OCT visualized well fine choroidal details, but only partially visualized the posterior vitreous architecture.

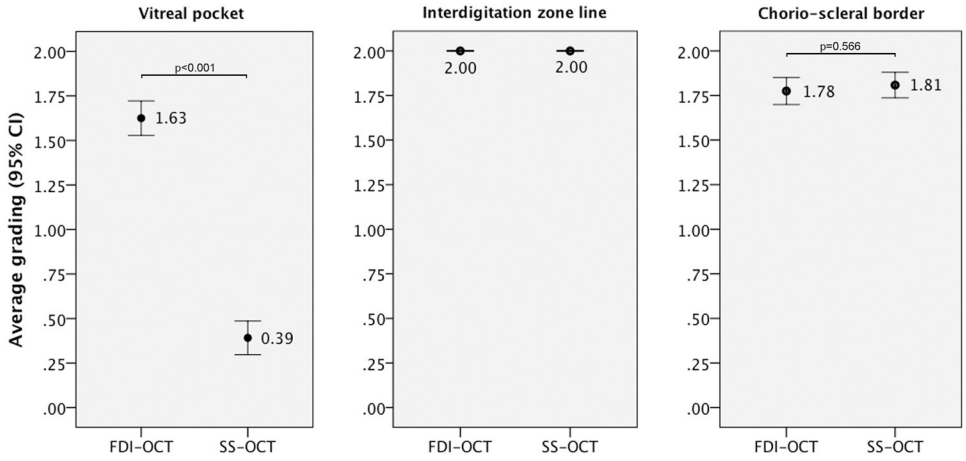

Figure 1.

Qualitative comparison of the FDI SD-OCT imaging to the SS-OCT imaging with respect to visualization of the anterior border of the premacular bursa, interdigitation zone line, and chorio-scleral boundary. The grading system was the following: grade 0 indicated that the structure was not seen, grade 1 indicated that the structure was barely seen, and grade 2 indicated that the structure was clearly seen. The scores were added for the two graders, who were masked to OCT imaging modality. Shown are average scores for each OCT modality with 95% confidence intervals.

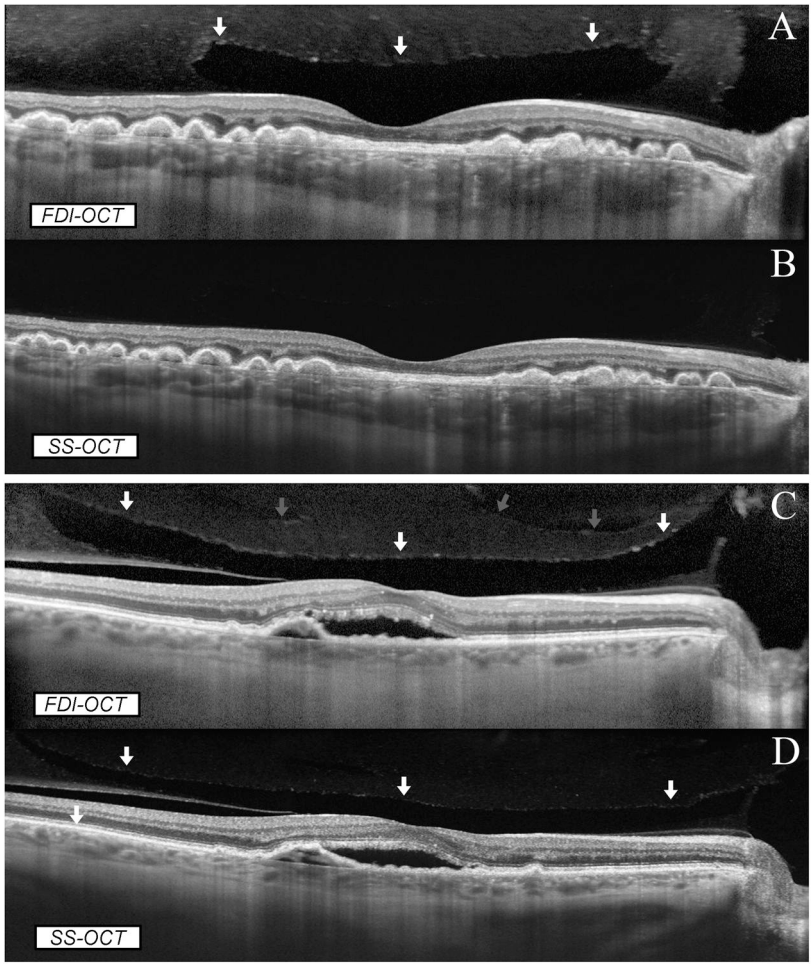

Figure 2.

Comparison between FDI SD-OCT and SS-OCT in full-depth visualization of posterior ocular structures. In an eye with dry AMD (A, B), both imaging modalities showed the full thickness of the retina and choroid. However, the premacular bursa was detected only on SD-OCT imaging (A; the arrows indicate the anterior border of the bursa) whilst it was not imaged by the SS-OCT (B). In an eye with wet AMD (C, D), both imaging modalities showed the full thickness of the retina and choroid. The anterior border of the premacular bursa was clearly seen on SD-OCT imaging (C, white arrows) whilst it was only barely seen on SS-OCT imaging (D, white arrows). In addition, SD-OCT imaging showed a more anterior vitreoschisis (C, grey arrows) that was missed on SS-OCT imaging (D).

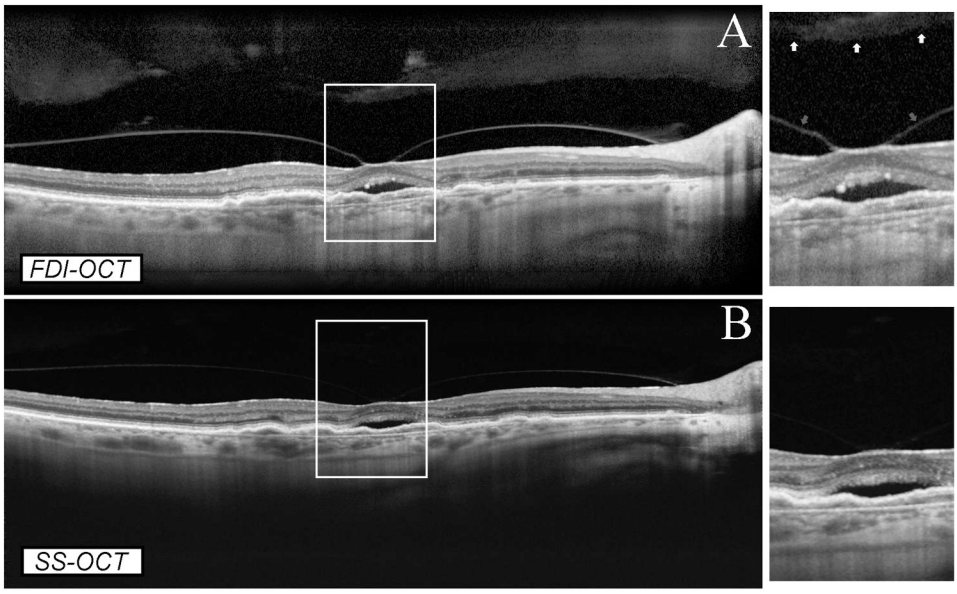

Figure 3.

Comparison between FDI SD-OCT (A) and SS-OCT (B) in full-depth visualization of posterior ocular structures in an eye with wet AMD. Both OCT modalities showed clearly the full thickness of the retina and choroid. However, SD-OCT imaging nicely showed the presence of the premacular bursa with vitreomacular traction, which was barely evident on SS-OCT imaging in magnified visualization.

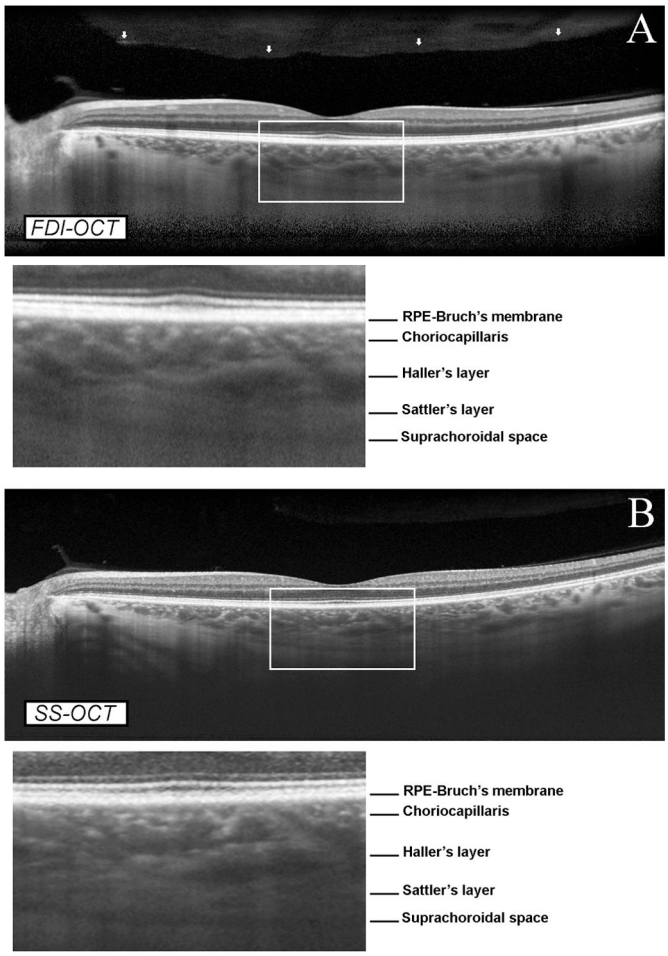

Figure 4.

Comparison between FDI SD-OCT (A) and SS-OCT (B) in full-depth visualization of posterior ocular structures in a normal eye. Both OCT modalities showed clearly the full thickness of the retina and choroid. SD-OCT imaging showed the presence of the premacular bursa, which was not evident on SS-OCT imaging. Both imaging modalities showed the five layers of the choroid, including Bruch's membrane, choriocapillaris, two vascular layers (Haller's and Sattler's), and the suprachoroidal space. However, the choroidal structures were sharper in the SS-OCT image (B) compared to the FDI SD-OCT image (A) in magnified visualization.